Kinetic Evidence for a Substrate-Induced Fit in Phosphonoacetaldehyde Hydrolase Catalysis†

Guofeng Zhang,‡ Andrew S. Mazurkie,§ Debra Dunaway-Mariano,*,‡ and Karen N. Allen*,§

Department of Chemistry, University of New Mexico, Albuquerque, New Mexico 87131, and Department of Physiology and Biophysics, Boston University School of Medicine, Boston, Massachusetts 02118-2394

Received July 1, 2002; Revised Manuscript Received August 15, 2002

ABSTRACT: Phosphonoacetaldehyde hydrolase (phosphonatase) from *Bacillus cereus* catalyzes hydrolytic P−C bond cleavage of phosphonoacetaldehyde (Pald) via a Schiff base intermediate formed with Lys53. A single turnover requires binding of Pald to the active site of the core domain, closure of the cap domain containing the Lys53 over the core domain, and dissociation of the products following catalysis. The ligand binding and dissociation steps occur from the "open conformer" (domains are separated and the active site is solvent-exposed), while catalysis occurs from the "closed conformer" (domains are bound together and the active site is sequestered from solvent). To test the hypothesis that bound substrate stabilizes the closed conformer, thus facilitating catalysis, the rates of chemical modification of Lys53 in the presence and absence of inert substrate and/or product analogues were compared. Acetylation of Lys53 with 2,4-dinitrophenylacetate (DNPA) resulted in the loss of enzyme activity. The pseudo-first-order rate constant for inactivation varied with pH. The pH profile of inactivation is consistent with a pK_a of 9.3 for Lys53. The inhibitors tungstate and vinyl sulfonate, which are known to bind to active site residues comprising the core domain, protected Lys53 from acetylation. These results are consistent with a dynamic equilibrium between the open and closed conformations of phosphonatase and the hypothesis that ligand binding stabilizes the closed conformation required for catalytic turnover.

Phosphonoacetaldehyde hydrolase (phosphonatase)[1] from *Bacillus cereus* catalyzes hydrolytic P−C bond cleavage in phosphonoacetaldehyde (Pald) to form acetaldehyde and orthophosphate (*2*) (Figure 1). The enzyme binds Mg(II) at each of the two active sites of its homodimeric structure. The enzyme-catalyzed reaction proceeds via a Schiff base intermediate, formed from Lys53 and the Pald carbonyl group (*3*, *4*), and a phosphoenzyme intermediate, formed by phosphoryl transfer from the Schiff base to Asp12 (*4*, *5*). Hydrolyses of the aspartyl phosphate and Lys-ϵ-ethylenamine groups release the respective products, orthophosphate and acetaldehyde.

X-ray crystallographic analysis of tungstate (a phosphate analogue)-soaked crystals of the phosphonatase−Mg(II) complex showed that the protein monomer is organized into a core domain and a cap domain connected by two, solvated peptide linker regions (*6*) (Figure 2). Both domains were found to contribute catalytic residues to the active site, which is located at the domain−domain interface. The core domain contributes the catalytic aspartate and residues which bind the Mg(II) and phosphoryl moiety of the substrate, while the cap domain contributes the Schiff base lysine and residues which surround the aldehydic portion of the substrate. The active site of one subunit was bound to Mg(II) only (Figure 2A), while the other was bound to Mg(II) and tungstate (Figure 2B). The relative orientations of the cap and core domains in these two subunits were different. The subunit which contained only the Mg(II) assumed an "open conformation" in which the two domains were separated and the active site crevice was solvated. The subunit which contained Mg(II) and tungstate was in a "closed conformation", in which the cap domain and core domain were closely associated and the active site was sequestered from solvent. A hinge-like motion between the two domains, acting as rigid bodies, produces the conversion of one enzyme conformer to the other. This movement is the result of changes in the backbone conformation of specific linker residues (highlighted in Figure 2).

On the basis of the two "snapshots" of phosphonatase derived from the crystallographic analysis, a dynamic, solution equilibrium between open and closed enzyme conformers can be envisioned. Substrate would thus bind to, and products would dissociate from, the open conformer, while catalysis would occur in the closed conformer. There

† This work was supported by NIH Grant GM61099 to K.N.A. and D.D.-M.

* To whom correspondence should be addressed. D.D.-M.: Department of Chemistry, University of New Mexico, Albuquerque, NM 87131; telephone, (505) 277-3383; fax, (505) 277-6202; e-mail, dd39@unm.edu. K.N.A.: Department of Physiology and Biophysics, Boston University School of Medicine, 80 E. Concord St., Boston, MA 02118-2394; telephone, (617) 638-4398; fax, (617) 638-4285; e-mail, allen@med-xtal.bu.edu.

‡ University of New Mexico.

§ Boston University School of Medicine.

[1] Abbreviations: Pald, phosphonoacetaldehyde; phosphonatase, phosphonoacetaldehyde hydrolase; DNPA, 2,4-dinitrophenyl acetate; CAPS, 3-(cyclohexylamino)-1-butanesulfonic acid; CHES, 2-(cyclohexylamino)ethane-2-sulfonic acid; TAPS, 3-{[tris(hydroxymethyl)-methyl]amino}propanesulfonic acid; HEPES, *N*-(2-hydroxyethyl)-piperazine-*N*′-2-ethanesulfonic acid; NADH, dihydronicotinamide adenine dinucleotide; DTT, dithiothreitol; MALDI-MS, matrix-assisted laser desorption ionization (time-of-flight) mass spectrometry.

10.1021/bi026388n CCC: $22.00
Published on Web 10/19/2002

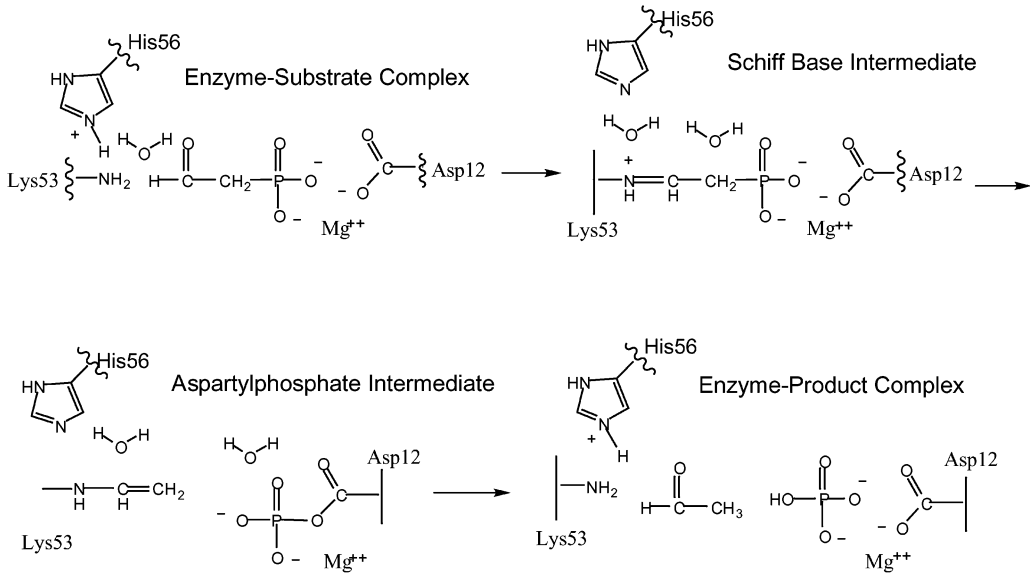

FIGURE 1: Reaction steps associated with the phosphonatase-catalyzed hydrolysis of Pald to acetaldehyde and orthophosphate.

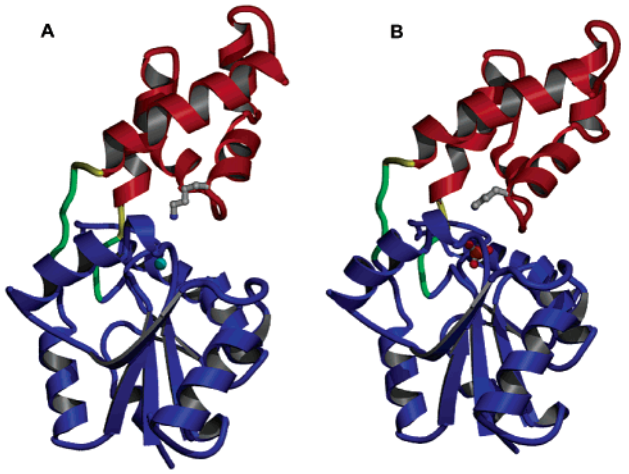

FIGURE 2: Three-dimensional structure of *B. cereus* phosphonatase (*6*). (A) Monomer of the enzyme−Mg(II) complex in the open conformation. (B) Monomer of the enzyme−Mg(II)−tungstate complex in the closed conformation. The protein is differentially colored as follows: red for the cap domain, blue for the core domain, green for linkers, yellow for hinges, gray for Lys53, cyan for Mg(II), and orange for tungstate.

are numerous examples of enzymes that employ domain−domain closure to desolvate the reaction site, and like phosphonatase, most employ hinge-like motions in peptide linkers to mediate domain−domain association and dissociation (*7*). Typically, bond rotations in peptide linkers are intrinsically fast, and the rates of domain−domain binding and dissociation are therefore governed by the rates of rigid body diffusion (*8*, *9*). The measured rate of phosphonatase catalysis ($k_{cat} = 15\ s^{-1}$; $k_{cat}/K_m = 5 \times 10^5\ M^{-1}\ s^{-1}$), which sets a minimum for the rate of the combined chemical steps, is slower than the rate of rigid body diffusion in water. Thus, unless an underlying mechanism for reducing the rate of domain diffusion exists, the phosphonatase active site may be opened to solvent before the chemistry has been completed.

To our knowledge, domain−domain association and dissociation rates have not yet been experimentally correlated with catalytic turnover rates, although the rates of active site loop movements have been (see refs *10* and *11*). In the scenario tested herein, the presence of bound substrate inhibits domain−domain dissociation and shifts the phosphonatase conformer equilibrium from the open conformer to the closed conformer. This variation on the classical induced fit model of enzyme catalysis (*12*) is well-precedented in the literature (for recent examples, see refs *13*−*16*).

To test the substrate-induced fit model in the phosphonatase catalytic mechanism, the effect of ligand binding (mediated by the core domain) on the solvent accessibility of Lys53 (contributed by the cap domain) was assessed. The pH dependence of the rate of acetylation of Lys53 by 2,4-dinitrophenylacetate (DNPA) was measured to determine the pK_a of Lys53. In addition, the rate of acetylation of the neutral Lys53 in the presence and absence of ligand was compared. The experimental approach used to determine the pK_a of Lys53 was inspired by the elegant studies of Schmidt and Westheimer (*17*). In that study, the pH dependence of acyl transfer from 2,4-dinitrophenyl propionate to the Schiff Base forming Lys115 of acetoacetate decarboxylase (*18*, *19*) was used to determine the pK_a of the Lys115 ϵ-ammonium group. Because acyl transfer could only occur with the neutral Lys115 ϵ-amine, the observed rate constant for the reaction varied with the fraction of the enzyme in the neutral form, according to eq 1 (*17*). The neutral fraction was determined by the pH of the reaction solution and by the acid dissociation constant (K_a) of the Lys115 ϵ-ammonium group. Therefore, the determination of the apparent rate constant (k_{obs}) as a function of pH allowed the determination of the pK_a of Lys115 from the inflection point in the plot of k_{obs} versus pH.

$$\begin{array}{ccccccc} \text{E-NH}_2 & + & \text{DNPA} & \xrightarrow{k} & \text{E-NH-Ac} & + & \text{DNP} \\ \mathrm{H^+}\ \updownarrow\ K_a & & & & & & \\ \text{E-NH}_3^+ & & & & & & \end{array} \qquad k_{obs} = k[\text{DNPA}]/(1+[\mathrm{H^+}]/K_a) \qquad (1)$$

Schmidt and Westheimer (*17*) found that the pK_a of Lys115 of acetoacetate decarboxylase is only 5.9, 4.6 pH

units lower than that reported for the ϵ-ammonium group of Lys in solution (pK_a = 10.5) (*20*). Additional titration studies, carried out with an active site-bound amine reporter group, corroborated this remarkable finding (*21*, *22*). Kokesh and Westheimer (*22*) hypothesized that the proximity of a Lys residue (Lys116) to Lys115 was responsible for the unique active site environment, and for the pK_a perturbation. This hypothesis was later supported by the mutagenesis-based studies of Highbarger et al. (*23*).

In phosphonatase, the Schiff base forming Lys53 would only be accessible to an acetylating agent in the open conformer. In addition, in the open conformer, Lys53 would be highly solvated and, thus, expected to have a pK_a similar to that of the ϵ-ammonium group of Lys in water (viz., 10.5), in stark contrast to the example of the Schiff base lysine of acetoacetate decarboxylase. In this paper, we report that the acetylation reaction of Lys53 with DNPA follows second-order kinetics, that the pH dependency of the observed rate constant defines a pK_a of 9.3, and that tungstate and vinyl sulfonate protect against acetylation. These results are consistent with the presence of a dynamic equilibrium between the open and closed conformations of phosphonatase and the hypothesis that ligand binding stabilizes the closed conformation required for catalytic turnover.

EXPERIMENTAL PROCEDURES

Materials. Pald was prepared according to the published procedure (*24*). DNPA was prepared from 2,4-dinitrophenol and acetyl chloride according to the published procedure (*17*). 2,4-Dinitrophenyl [D_3]acetate was prepared using [D_3]acetyl chloride (Sigma-Aldrich). Wild-type phosphonatase was prepared as described in ref *4*, while the C22S mutant was prepared as described in ref *25*. Recombinant *Clostridium acetobutylicum* acetoacetate decarboxylase expressed in *Escherichia coli* was prepared as previously described (*23*). L-1-Tosylamide-2-phenylethyl chloromethyl ketone-treated trypsin from bovine pancreas, Baker's yeast alcohol dehydrogenase, NADH, and buffers were purchased from Sigma. The molecular graphics program O (*26*) was used for manual docking of DNPA to phosphonatase (PDB entry 1FEZ) on a Silicon Graphics O2 Modeler. The model for the DNPA was generated using the program QUANTA (MSI).

pH Profiles for DNPA Inactivation. To check for interference of active site residue C22 with labeling of the Schiff base lysine, the mutant C22S was used instead of wild-type phosphonatase (as noted) in some inactivation experiments. Inactivation reactions were initiated by adding 6−50 μL of 10 mM DNPA (in spectrograde acetonitrile) to a 994−950 μL, 0 °C solution of buffer (10 mM TAPS and 90 mM CHES for pH 8−9, 100 mM CHES for pH 8.5−10, and 10 mM CAPS and 90 mM CHES for pH 9.5−11) containing 10 mM $MgCl_2$ and enzyme (5−10 μM wild-type phosphonatase, 50 μM C22S phosphonatase, or 7 μM acetoacetate decarboxylase). For the protection experiments, inactivation reactions were carried out in 100 mM CHES (pH 9.0, 0 °C) containing 400 μM DNPA and 50 μM C22S phosphonatase in the presence of tungstate (0−0.9 mM) or vinyl sulfonate (0−1.5 mM). After a specified period of time, a 10 μL aliquot of the inactivation reaction mixture was transferred to a 1 mL assay solution containing 100 mM K^+HEPES (pH 7.0), 5 mM $MgCl_2$, 400 μM Pald (saturating), 0.3 mM NADH, and 10 units of alcohol dehydrogenase at 25 °C. The initial velocity of the reaction was monitored by measuring the decrease in absorption at 340 nm associated with the oxidation of NADH to NAD ($\Delta\epsilon$ = 6.22 mM^{-1} cm^{-1}). The acetoacetate decarboxylase inactivation reaction mixture was transferred to a 1 mL assay solution containing 40 mM acetoacetate (saturating) in 100 mM K^+HEPES (pH 7.0) at 25 °C. The initial velocity of the reaction was monitored by measuring the decrease in solution absorption at 270 nm (*23*). For both the phosphonatase and acetoacetate decarboxylation assays, the initial velocity of the catalyzed reaction was assumed to equal the maximum velocity, and hence, the ratio of the initial velocity and the enzyme concentration was assumed to be k_{cat}. The ratio of k_{cat} for enzyme incubated with DNPA for a specified time t (k_t) and the k_{cat} of enzyme incubated in buffer without DNPA (k_o) was plotted against t. The observed pseudo-first-order rate constant for inactivation (k_{inact}) was calculated from the negative slope of the plot of ln k_t/k_o versus t. The pK_a was calculated from the pH dependence of k_2 using eq 2 and the computer program KaleidaGraph or KinetAsyst.

$$\log Y = \log[Y_L + Y_H(K/[H])/(1 + K/[H])] \qquad (2)$$

where K is the acid dissociation constant, Y is the observed k_{inact} at the hydrogen ion concentration [H], and Y_L and Y_H are the minimum and maximum values of k_{inact}, respectively.

Protection by Tungstate and Vinyl Sulfonate. The observed k_{inact} for the inactivation reaction of C22S phosphonatase and DNPA was measured at varying concentrations of inhibitor [tungstate (0−0.9 mM) or vinyl sulfonate (0−1.5 mM)]. Inactivation solutions contained 50 μM C22S phosphonatase, 400 μM DNPA, and varying concentrations of tungstate (0−0.9 mM) or vinyl sulfonate (0−1.5 mM) in 100 mM CHES (pH 9.0, 0 °C). The k_{inact}, determined as described in the previous section, was plotted as a function of inhibitor concentration.

The titration curves were fitted to eq 3 using the Kaleida Graph computer program for nonlinear regression analysis.

$$\Delta k = k_o + (\Delta k_{max}/[E])\{K_d + [E] + [I] - [(K_d + [E] + [I])^2 - 4[E][I]]^{1/2}\}/2 \qquad (3)$$

where [I] is the total inhibitor concentration, [E] is the total enzyme concentration, K_d is the apparent dissociation constant of the enzyme−inhibitor complex, Δk is the observed change in the rate constant, Δk_{max} is the maximum change in the rate constant, and k_o is the initial rate constant without inhibitor.

MALDI Mass Spectral Analysis of Trypsin Digests of DNPA-Treated Phosphonatase. MALDI mass spectra were measured at the Cornell University Weill Medical College Mass Spectrometry Facility. Samples were prepared by reacting 500 μM 2,4-dinitrophenyl [1-H_3]acetate or a mixture of 250 μM 2,4-dinitrophenyl [1-H_3]acetate and 250 μM 2,4-dinitrophenyl [1-D_3]acetate 2,4-dinitrophenylacetate with 50 μM C22S phosphonatase in a 4 mL solution of 100 mM CHES buffer (pH 9.0) containing 10 mM $MgCl_2$ for 30 min at 0 °C. Reactions were terminated by adding 46 mL of 50 mM K^+HEPES (pH 7.0, 0 °C) containing 5 mM $MgCl_2$. The resulting solutions were exhaustively dialyzed against 50 mM K^+HEPES (pH 7.0, 4 °C) containing 5 mM $MgCl_2$ and then

concentrated in a 10 kDa cutoff centrifugal concentrator device (Pall Filtron Corp.) at 6500 rpm and 4 °C to a final volume of 4 mL. The protein samples were then transferred to 0.1 M NH_4HCO_3 (pH 7.8) by five consecutive cycles of dilution with buffer followed by concentration. The final concentration of protein in each sample was ~0.9 mg/mL. The trypsin digestion of each sample was carried out by the following procedure. A 1 mL aliquot was mixed with 0.75 μL of 1 M DTT and the mixture incubated at 50 °C for 30 min. The mixture was cooled to 37 °C, and trypsin (1:20 protein weight ratio) was added. After 5 h, the reaction was terminated by the addition of 2 volumes of 5% trifluoroacetic acid. Samples were stored at −80 °C until they were analyzed by MADLI-MS.

Preparation of K183A, K183L, and K121R/K146R/K192R Phosphonatases. The mutant genes were generated by the polymerase chain reaction using the plasmid pKK223-3, containing the wild-type phosphonatase gene as a template (*4*), and commercial oligonucleotides as primers. The PCR products were digested with *Eco*RI and *Pst*I restriction enzymes, and the desired DNA fragments were purified by agarose gel chromatography and then ligated into the pKK223-3 vector plasmid (digested with the same restriction enzymes) using T4 DNA ligase. The resulting clone was transformed into competent *E. coli* JM109 cells for gene expression. The sequence of each mutant was verified by commercial DNA sequencing (Center for Genetics in Medicine, University of New Mexico School of Medicine, Albuquerque, NM). The triple mutant K121R/K146R/K192R gene was constructed stepwise by PCR (*4*). The K121R mutant was first constructed using the wild-type gene as a template; the K121R/K146R double mutant was constructed using the K121R gene as a template, and finally, the K121R/K146R/K192R triple mutant was constructed using the K121R/K146R gene as a template.

The K183A, K183L, and K121R/K146R/K192R phosphonatase mutants were purified using the same procedure used to purify the wild-type enzyme (*4*) in yields of 10, 20, and 6 mg/g of wet cells, respectively. The purity of each mutant enzyme was confirmed by SDS−PAGE analysis. It was observed that the chromatographic behavior, solubility, and stability to storage of the mutants were similar to those of the wild-type enzyme.

Steady-State Kinetic Constants. The K_m and V_{max} values for wild-type and mutant phosphonatases were determined from the initial velocity data measured as a function of Pald concentration ($0.5-10K_m$). The 1 mL reaction solutions contained Pald, 10 mM $MgCl_2$, 0.15 mM NADH, and 5 units of alcohol dehydrogenase in 50 mM K^+HEPES (pH 7.5, 25 °C). Reactions were monitored at 340 nm ($\Delta\epsilon = 6200$ M^{-1} cm^{-1}) for conversion of acetaldehyde and NADH to ethanol and NAD (*4*). Inhibition constants were determined by measuring the initial velocities of C22S phosphonatase-catalyzed reactions carried out in 100 mM K^+HEPES buffer (pH 7.5, 25 °C) in the presence of 0, 100, 150, and 200 μM tungstate or 0, 100, 250, and 500 μM vinyl sulfonate. The initial velocity data were analyzed using eqs 4 and 5.

$$V_o = V_{max}[A]/(K_m + [A]) \quad (4)$$

$$V_o = V_{max}[A]/[K_m(1 + [I]/K_i) + [A]] \quad (5)$$

where [A] is the substrate concentration, [I] is the inhibitor concentration, V_o is the initial velocity, V_{max} is the maximum velocity, K_m is the Michaelis constant, and K_i is the inhibitor concentration. The k_{cat} was calculated from V_{max} and the enzyme concentration by using the equation $k_{cat} = V_{max}/[E]$. The enzyme concentration was determined using the Bradford method (*27*).

RESULTS

pH Dependence of Enzyme Inactivation with 2,4-Dinitrophenyl Acetate. The plots of the pH dependencies of the observed rate constants for DNPA inactivation (k_{inact}) of recombinant *B. cereus* wild-type and C22S mutant phosphonatase and *C. acetobutylicum* acetoacetate decarboxylase at 0 °C are shown in Figure 3. The pK_a values derived from the pH profiles measured for wild-type and C22S mutant phosphonatases are essentially identical: 9.32 ± 0.05 and 9.27 ± 0.04, respectively. The Cys22 thiol group projects into the active site. Its ionization, which is expected to occur at alkaline pH [the pK_a of the solvated cysteine thiol is 8.4 (*21*)], might have influenced the outcome of the pK_a determination. To rule out this possibility, the C22S mutant [which retains 10% of the catalytic activity of the wild-type phosphonatase (*25*)] was subjected to the same pH profile analysis as the wild-type enzyme.

The pH profile of k_{inact} for DNPA inactivation of acetoacetate decarboxylase was measured for comparison to that of phosphonatase (Figure 3). The pK_a of 6.4 ± 0.1 measured with DNPA at 0 °C is close, but (because of the lower temperature)[2] not identical, to the pK_a of 5.9 derived from the pH−rate profile of the acylation of Lys in acetoacetate decarboxylase by 2,4-dinitrophenylproprionate at 30 °C (*17*). It is quite different in value, however, from the pK_a of 9.3 measured for phosphonatase. Whereas the microenvironment of the phosphonatase essential Lys causes a small perturbation in pK_a (1 pH unit), that of the acetoacetate decarboxylase changes the K_a by 4 orders of magnitude (pK_a decreased by 4 pH units).

Mutagenesis of an Active Site Lysine Residue. In phosphonatase, there are two active site Lys residues: the Schiff base-forming Lys53 of the cap domain and Lys183 of the core domain (*6*). Although Lys183 is too far removed from the reaction center to contribute directly to catalysis (Figure 4), it is stringently conserved. Therefore, it is likely that the charged Lys183 side chain plays an important role in maintaining the integrity of the active site environment [where it forms a salt bridge with the side chain of Asp190, which in turn binds to a water ligand of the Mg(II) cofactor]. To determine if phosphonatase catalysis is impaired by the loss of Lys183 function, site-directed mutagenesis was used to replace Lys183 with Ala or Leu. The kinetic constants of the two mutants are compared with that of wild-type phosphonatase in Table 1. The activity of the K183L mutant, in which the space filling property of the Lys side chain is largely preserved, is greater than that of the K183A mutant. However, both mutants are significantly less active than wild-type phosphonatase (k_{cat} reduced by a factor of $3-12 \times 10^2$ and k_{cat}/K_m reduced by a factor of 1×10^3 to 1×10^4). Thus,

[2] The enthalpy of ionization of a lysine ϵ-ammonium group is ca. 10 kcal/mol (*1*), and thus, the experimental pK_a is larger when measured at 0 °C than when measured at 30 °C.

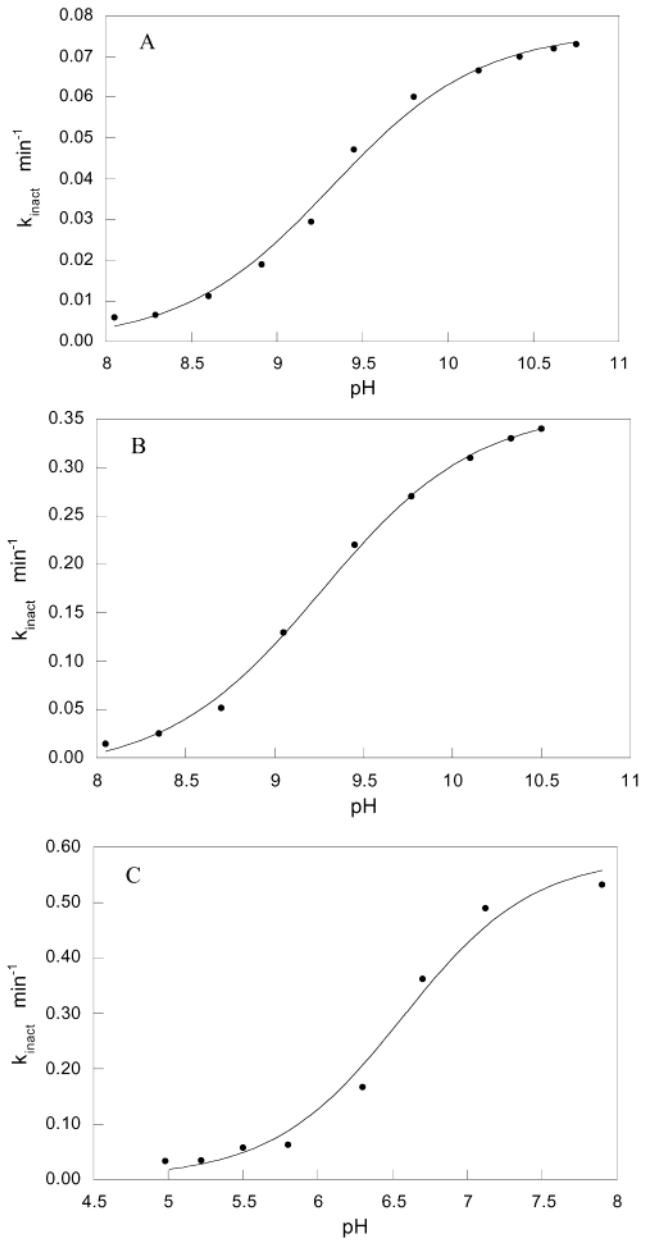

FIGURE 3: Plot of the observed rate constant for inactivation (k_{inact}) vs solution pH. (A) Reaction of 10 μM wild-type phosphonatase, 10 mM $MgCl_2$, and 100 μM DNPA. (B) Reaction of 50 μM C22S phosphonatase, 10 mM $MgCl_2$, and 400 μM DNPA. (C) Reaction of 7 μM acetoacetate decarboxylase and 60 μM DNPA. The data were fitted with eq 2. See Experimental Procedures for details.

a loss of catalytic activity upon acetylation of Lys183 is expected. The pK_a consistent with the pH profile shown in Figure 3 could, therefore, have been attributed to Lys53 or Lys183. Further experimentation was necessary to determine which residue was acetylated by the DNPA.

MALDI-MS Analysis of Acetylated Phosphonatase. Acetylation of phosphonatase adds 42 Da to the subunit mass of 30 361 Da. The fractional increase in mass is too small to reliably detect by electron spray mass spectrometry. Instead, MALDI-MS analysis of trypsin digests of DNPA-treated C22S phosphonatase was utilized to identify the Lys residues acetylated by DNPA (use of the wild-type enzyme would be expected to yield the same result). The sample that was utilized was produced by the reaction of 50 μM enzyme with 500 μM DNPA at pH 9.0 and 0 °C for 30 min, reaction

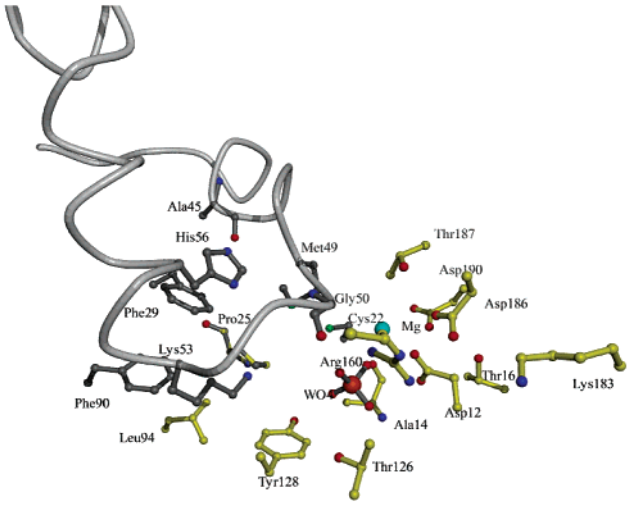

FIGURE 4: Active site structure of the enzyme−Mg(II)−tungstate complex in the closed conformation (*6*). The following features are highlighted by color: the α-helix from the cap domain and residues from the cap domain in gray, residues from the core domain in yellow, Mg(II) as a cyan-colored sphere, and the tungstate in orange.

Table 1: Steady-State Kinetic Constants Determined for Wild-Type and Mutant Phosphonatase at pH 7.0 and 25 °C

phosphonatase	k_{cat} (s^{-1})	K_m (μM)	k_{cat}/K_m (s^{-1} M^{-1})
wild-type	15 ± 1	33 ± 2	4.6×10^5
K183A	0.0120 ± 0.002	770 ± 30	1.6×10
K183L	0.046 ± 0.007	193 ± 8	2.4×10^2

```
     1   *    10   *    20   *    30   *    40   *    50
1    MDRMKIEAVIFDWAGTTVDYGSFAPLEVFMEIFHKRGVAITAEEARKPMG
51   LLKIDHVRALTEMPRIASEWNRVFRQLPTEADIQEMYEEFEEILFAILPR
101  YASPINAVKEVIASLRERGIKIGSTTGYTREMMDIVAKEAALQGYKPDFL
151  VTPDDVPAGRPYPWMCYKNAMELGVYPMNHMIKVGDTVSDMKEGRNAGMW
201  TVGVILGSSELGLTEEEVENMDSVELREKIEVVRNRFVENGAHFTIETMQ
251  ELESVMEHIEKNELIIS
```

FIGURE 5: Amino acid sequence of *B. cereus* phosphonatase (Lys53 underlined). Trypsin cleavage sites are C-terminal to Arg and unacetylated Lys residues. Peptide fragments containing acetylated Lys that were identified by MALDI-MS analysis are highlighted in yellow. The observed peptide fragment containing unmodified Lys183 is highlighted in lime green.

conditions which result in complete inactivation of the enzyme. The tryptic digest of the modified enzyme was then subjected to MALDI-MS analysis. Because phosphonatase contains numerous Lys and Arg residues, the number of peptides that can be generated by trypsin digestion is large (29 to be exact; see the sequence in Figure 5). However, only peptides in the molecular mass range of 500−3000 Da are suitable for detection by MALDI-MS analysis, and some fragments in this mass range will go undetected. However, the two fragments that contained Lys53 and Lys183 were observed in the MALDI mass spectrum of the digested protein.

Of the 13 Lys residues present in phosphonatase, only Lys5, Lys53, Lys121, Lys138, Lys146, Lys183, and Lys192 are located in the active site or on the protein surface, and thus are potentially reactive with DNPA. To identify the peptide fragments containing acetylated Lys in the mass spectrum, a deuterium labeling strategy was employed. Accordingly, the enzyme was reacted with a 1:1 mixture of 2,4-dinitrophenyl [1-H_3]acetate and 2,4-dinitrophenyl [1-D_3]-

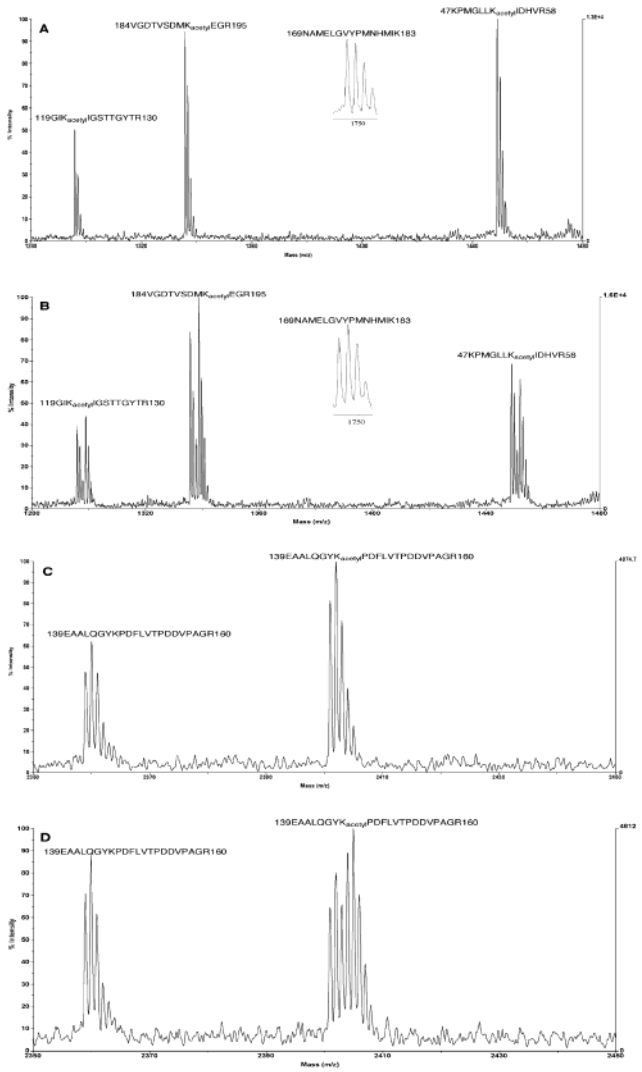

FIGURE 6: MALDI-MS data from analysis of the peptide fragments generated by trypsin digestion of C22S phosphonatase reacted with (A and C) 2,4-dinitrophenyl [H_3]acetate and (B and D) a 1:1 mixture of 2,4-dinitrophenyl [H_3]acetate and 2,4-dinitrophenyl [D_3]acetate.

acetate and then subjected to tryptic digestion and MALDI-MS analysis as previously described. The three deuterium atoms of the deuterated acetyl group added 3 Da to the mass of the acetylated peptide fragment. Thus, two equal-sized peaks separated by 3 Da were observed for each acetylated fragment.

As shown in Figure 6, four acetylated peptides were detected, the *m*/*z* values of which are listed in Table 2. The following peptides contained acetylated Lys residues: ^{47}KPMGLL$\underline{\text{K}}^{53}$(acetyl)IDHVR^{58}, ^{119}GIK^{121}(acetyl)-IGSTTGYTR^{130}, ^{184}VGDTVSDMK^{192}(acetyl)EGR^{195}, and ^{139}-EAALQGYK^{146}(acetyl)PDFLVTPDDVPAGR^{160} (although only ~50% of the protein was acetylated at the Lys146 residue). Aside from Lys53, only Lys121 is conserved and, thus, conceivably responsible for activity loss. In addition, unlike Lys53, residues Lys121, Lys192, and Lys146 are far from the active site and, thus, not subject to protection by active site ligands (see a following section). Nevertheless, to unambiguously show that the acetylations of Lys121, Lys146, and Lys192 are *not* responsible for the activity loss in DNPA-treated phosphonatase, the triple mutant K121R/K146R/K192R was prepared (k_{cat} = 1.28 ± 0.01 s^{-1} and K_m = 56 ± 2 μM). The k_{inact} values for wild-type and K121R/K146R/K192R phosphonatase measured under identical conditions (viz., 10 μM enzyme, 100 μM DNPA, pH 9.3, and 0 °C) were 0.011 and 0.012 s^{-1}, respectively. Measured in the presence of 1 mM tungstate, the values of k_{inact} were reduced to 0.003 s^{-1} (see the protection experiments in a following section).

Table 2: Calculated and Measured *m*/*z* Values of Trypsin-Generated Peptide Fragments from Acetylated Phosphonatase[a]

acetylated fragment	mass (*m*/*z*) calculated (H/D)	measured (H/D)
119−130	1295.422/1298.422	1295.882/1298.867
		1296.885/1299.866
		1297.827/1330.858
184−195	1335.421/1338.421	1335.798/1338.778
		1336.798/1339.777
		1337.799/1340.782
47−58	1448.759/1451.759	1448.944/1451.960
		1449.948/1452.960
		1450.961/1453.963

50% acetylated fragment	mass (*m*/*z*) calculated (no/H or D)	measured (no/H/D)
139−160	2359.622/2401.622	2359.045/2401.033
		2360.028/2402.032
		2361.031/2403.035
	2359.622/2404.622	2359.956/2401.962/2404.970
		2360.940/2402.959/2405.977
		2361.930/2403.970/2406.980

unacetylated fragment	mass (*m*/*z*) calculated	measured
169−183	1748.125	1747.857/1748.866/1749.876

[a] See Experimental Procedures for details.

Finally, acetylation of Lys183 was ruled out on the basis of the observation of the 1748 peak in the MALDI mass spectrum of the digested acetylated protein. This peak corresponds to the fragment ^{169}NAMELGVYPMNHMI**K**^{183}, in which Lys183 is *not* acetylated. Moreover, the 1790/1793 peaks, which would correspond to the proteo and deutero acetylated Lys183 fragment, were *not* present. Thus, Lys183 was not acetylated by the DNPA reaction,[3] and therefore, Lys183 could not be responsible for the observed activity loss. In conclusion, it is the acetylation of Lys53 that results in the loss of enzyme activity, and it is the pK_a of Lys53 that was measured in the pH profile shown in Figure 3.

Kinetics of Inactivation. The rate constant for inactivation of wild-type phosphonatase (10 μM) at pH 9.3 and 0 °C was measured as a function of DNPA concentration (0−200 μM) under pseudo-first-order conditions. The linear relationship observed between DNPA concentration and k_{inact} (see Figure 7) was compatible with a simple bimolecular reaction. The slope of the plot defined the bimolecular rate constant (k_2) to be 230 M^{-1} min^{-1}. There was *no* evidence found for a pre-equilibrium binding step in which the DNPA associates with the enzyme to form an enzyme−DNPA complex prior to acetylation of Lys53. Manual docking experiments showed that the enzyme could not attain the

[3] The absence of acetylation at Lys183, located on the core domain, can be rationalized from the solvent accessible surface calculation for the protein. The Lys183 ϵ-amine group is not solvent-exposed and, thus, is inaccessible for reaction with DNPA.

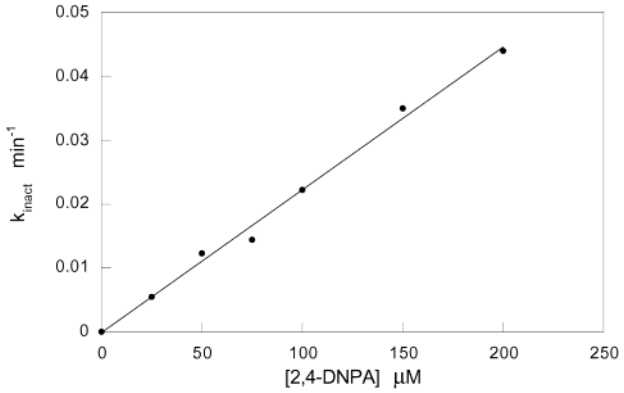

FIGURE 7: Plot of the observed rate constant for inactivation (k_{inact}) vs DNPA concentration. Reactions were carried out in 100 mM CHES buffer (pH 9.3) containing 10 μM wild-type phosphonatase and 10 mM $MgCl_2$ at 0 °C. The data were fit with a linear equation.

closed conformation with DNPA ligand bound to the active site before reacting. Thus, the reasonable conclusion drawn from these findings is that the DNPA reacts with the solvated Lys53 by collision.

Core Domain Ligand Protection Experiments. X-ray crystallographic studies have shown that tungstate (a phosphate analogue) (*6*) and vinyl sulfonate (a Pald analogue) (*28*) bind to the active site of the core domain. At pH 9.0 and 25 °C, these ligands are competitive inhibitors versus the substrate Pald with K_i values of 83 ± 11 and 180 ± 20 μM (measured using C22S phosphonatase), respectively. Here, we tested the ability of these ligands to protect against inactivation of C22S phosphonatase by DNPA at pH 9.0 and 0 °C. Plots of the k_{inact} versus tungstate or vinyl sulfonate concentration are shown in Figure 8. Both ligands afforded protection. The titration curves were fitted with eq 3 (see Experimental Procedures) to obtain the dissociation constants for tungstate (K_d = 72 ± 5 μM) and vinyl sulfonate (K_d = 235 ± 30 μM). These values are equivalent to the K_i values derived from competitive inhibition of C22S phosphonatase catalysis. This result, in combination with the X-ray structures of the phosphonatase−tungstate and phosphonatase−vinyl sulfonate complexes (*6*, *28*), shows that tungstate and vinyl sulfonate protect against Lys53 acetylation by binding to the active site of the core domain.

DISCUSSION

Protection against Lys53 Acetylation Afforded by Substrate and/or Product Analogues as Evidence for an "Induced Fit Mechanism" of Catalysis. Although several of the Lys residues (Lys53, Lys121, Lys146, and Lys192) are acetylated by DNPA, only the acetylation of Lys53 results in activity loss. Thus, the plot of k_{inact} versus pH measures the pK_a of Lys53 and no other Lys residue. Furthermore, the reaction between the DNPA and Lys53 is governed by simple diffusion, and not by a prebinding step involving enzyme and reagent. Thus, tungstate and vinyl sulfonate binding to the core domain protects against Lys53 acetylation not by displacing bound DNPA but by binding to the open enzyme conformer and shifting the conformer equilibrium in favor of the closed conformer. Only in the open conformer is Lys53 accessible to the DNPA, and therefore, this shift in equilibrium will decrease the effective concentration of Lys53 available for reaction and, hence, decrease the reaction rate.

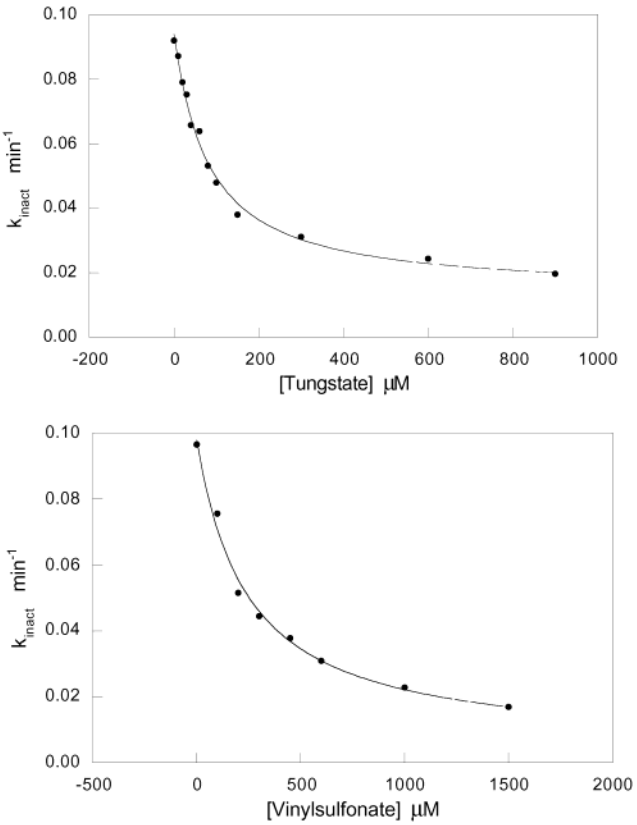

FIGURE 8: Plot of the observed rate constant for inactivation (k_{inact}) vs tungstate concentration (A) or vinyl sulfonate concentration (B). Reactions were carried out in 100 mM CHES (pH 9.0) containing 10 mM $MgCl_2$, 50 μM C22S phosphonatase, and 400 μM DNPA. The data were fit with eq 3.

In the closed conformation of the enzyme−ligand complex, the ligand phosphoryl group [as deduced from the binding of the phosphoryl analogues vinyl sulfonate and tungstate] binds to the guanidinium group of the core domain Arg160, which in turn binds to the backbone main chain carbonyl of the cap domain Gly50 (Figure 4) (*6*). It is conceivable that the bound ligand decreases the rate of domain−domain dissociation by bridging the network of stabilizing hydrogen bonds between the cap and core domains. The negatively charged group of the bound ligand may also contribute favorably to the electrostatic interactions that occur between active site residues in the closed conformer [i.e., neutralizing the charge of the bound Mg(II)]. Together, these effects may form the basis of substrate-induced fit in phosphonatase catalysis.

Differential Electronic Environments of Lys53 in the Open and Closed Conformations. The pK_a of Lys53 in the open enzyme conformer is 9.3. This pK_a is ∼1 pH unit lower than expected for the ϵ-ammonium group of lysine. Although Lys53 is solvated, it is located at the N-terminus of an α-helix (Figure 4) where it may experience unfavorable electrostatic interaction with the positive pole of the macrodipole [for example, the pK_a of protonated His located at the N-terminus of an α-helix is decreased by 0.8 pH unit (*29*)]. This interaction alone, or in combination with the local electrostatic potential (*30*) (the GRASP representation of the cap domain surface reveals a concentration of positive charge), may account for the perturbed pK_a.

Phosphonatase has a pH optimum at neutral pH (*31*). At this pH, Lys53 will be protonated. Following substrate

binding, the enzyme is stabilized in the closed conformation. When the cap and core domain are bound together, Lys53 is surrounded by hydrophobic active site residues (Figure 4). At this point, proton transfer may occur from the protonated Lys53 to the imidazole ring of His56, which is located in a polar microenvironment and forms a hydrogen bond to the backbone carbonyl of Ala45. The protonated histidine may then act as an acid catalyst in the subsequent departure of the hydroxyl group from the carbinolamine intermediate (formed by addition of the neutral Lys53 to the substrate carbonyl). To test this hypothetical reaction scheme, kinetic, structural, and mutagenesis studies will be utilized in future studies to assess the participation of the active site residues in catalysis.

REFERENCES

1. Cleland, W. W. (1977) *Adv. Enzymol. 45*, 273.
2. La Nauze, J. M., and Rosenberg, H. (1968) *Biochim. Biophys. Acta 165*, 438.
3. Olsen, D. B., Hepburn, T. W., Moos, M., Mariano, P. S., and Dunaway-Mariano, D. (1988) *Biochemistry 27*, 2229.
4. Baker, A. S., Ciocci, M. J., Metcalf, W. W., Kim, J., Babbitt, P. C., Wanner, B. L., Martin, B. M., and Dunaway-Mariano, D. (1998) *Biochemistry 37*, 9305.
5. Lee, S.-L., Hepburn, T. W., Swartz, W. H., Ammon, H. L., Mariano, P. S., and Dunaway-Mariano, D. (1992) *J. Am. Chem. Soc. 114*, 7346.
6. Morais, M. C., Zhang, W. H., Baker, A. S., Zhang, G. F., Dunaway-Mariano, D., and Allen, K. N. (2000) *Biochemistry 39*, 10385.
7. Hayward, S. (1999) *Proteins 36*, 425.
8. Gerstein, M., Lesk, A. M., and Cothia, C. (1994) *Biochemistry 33*, 6739.
9. McCammon, J. A., and Harvey, S. C. (1987) *Dynamics of Proteins and Nucleic Acids*, Cambridge University Press, New York.
10. Rozovsky, S., Jogl, G., Tong, L., and McDermott, A. E. (2001) *J. Mol. Biol. 310*, 271.
11. Osborne, M. J., Schnell, J., Benkovic, S. J., Dyson, H. J., and Wright, P. E. (2001) *Biochemistry 40*, 9846.
12. Koshland, D. E., Jr. (1958) *Proc. Natl. Acad. Sci. U.S.A. 44*, 98.
13. Li, F., Gangal, M., Juliano, C., Gofain, E., Taylor, S., and Johnson, A. (2002) *J. Mol. Biol. 315*, 459−469.
14. Szilagyi, A. N., Ghosh, M., Garman, E., and Vas, M. (2000) *J. Mol. Biol. 306*, 499.
15. Razeto, A., Kochhar, S., Hottinger, H., Dauter, M., Wilson, K. S., and Lamzin, V. S. (2002) *J. Mol. Biol. 318*, 109.
16. Thoden, J. B., Wesenberg, G., Raushel, F. M., and Holden, H. M. (1999) *Biochemistry 38*, 2347.
17. Schmidt, D. E., and Westheimer, F. H. (1971) *Biochemistry 10*, 1249.
18. Laursen, R. A., and Westheimer, F. H. (1966) *J. Am. Chem. Soc. 88*, 3426.
19. Pederson, D. J., and Bennett, G. N. (1993) *Gene 123*, 93.
20. Voet, D., and Voet, J. G. (1995) *Biochemistry*, p 59, Wiley, New York.
21. Frey, P. A., Kokesh, F. C., and Westheimer, F. H. (1971) *J. Am. Chem. Soc. 93*, 7266.
22. Kokesh, F. C., and Westheimer, F. H. (1971) *J. Am. Chem. Soc. 93*, 7270.
23. Highbarger, L. A., Gerlt, J. A., and Kenyon, G. L. (1996) *Biochemistry 35*, 41.
24. Isbell, A. F., Englert, L. F., and Rosenberg, H. (1969) *J. Org. Chem. 34*, 755.
25. Morias, M. C., Allen, K. N., Zhang, G., Zhang, W., and Dunaway-Mariano, D. (2002) *J. Biol. Chem.* (submitted for publication).
26. Kleywegt, G. J., and Jones, T. A. (1994) *Acta Crystallogr. D50*, 178−185.
27. Bradford, M. (1976) *Anal. Biochem. 72*, 248.
28. Lahiri, S. D., Morais, M. C., Allen, K. N., Zhang, G., Zhang, W. H., Olsen, D. B., and Dunaway-Mariano, D. (2002) unpublished data.
29. Sancho, J., Serrano, L., and Fersht, A. R. (1992) *Biochemistry 31*, 2253.
30. Fersht, A. (1999) *Structure and Mechanism in Protein Science*, p 179, W. H. Freeman and Co., New York.
31. Olsen, D. B., Hepburn, T. W., Lee, S.-L., Martin, B. M., Mariano, P. S., and Dunaway-Mariano, D. (1992) *Arch. Biochem. Biophys. 296*, 144.

BI026388N